Journal of Engineering Science and Technology
Vol. 13, No. 2 (2018) 295 - 308

INFLUENCE OF PULSED ELECTROPHORETIC DEPOSITION OF GRAPHITIC CARBON NANOTUBE ON ELECTROCHEMICAL CAPACITOR PERFORMANCE

KOK-TEE LAU[1,*], MOHD ASYADI AZAM[2],
RAJA NOOR AMALINA RAJA SEMAN[2]

[1]Carbon Research Technology Research Group, Faculty of Engineering Technology, Universiti Teknikal Malaysia Melaka, Hang Tuah Jaya, 76100 Durian Tunggal, Melaka, Malaysia
[2]Carbon Research Technology Research Group, Faculty of Manufacturing Engineering, Universiti Teknikal Malaysia Melaka, Hang Tuah Jaya,76100 Durian Tunggal, Melaka, Malaysia
*Corresponding email: ktlau@utem.edu.my

Abstract

Carbon nanotube (CNT)-based electrochemical capacitor (EC) has been actively studied as a high-power density energy storage for the portable product and energy sustainable development. The present work reports the deposit yields and graphitic concentration of CNT deposited by pulsed electrophoretic deposition (EPD) for the use as EC's active electrode materials. Using a conventional EPD apparatus, the pulsed EPD was conducted at pulse separation times (pause widths) of 30 to 50 s, alternated with the pulse width of 2.5 min. SEM micrograph showed the pulsed EPD at the pulse separation time of 30 s reduced the deposited CNT coating's density. An increase of the graphitic concentration by 40% as compared to the CNT coating deposited by continuous EPD was indicated by the I_G/I_D ratio of the Raman spectra results. The enrichment of graphitic phase in the EC drastically enlarged the specific capacitance of the EC by 150% as compared to the continuous EPD's EC result. The finding opens up the possibility of EC performance enhancement by controlling the graphitic CNT concentration of the electrode materials using pulse EPD process.

Keywords: Specific capacitance, Carbon nanotube, Graphitic carbon, Electrode materials, Electrophoretic deposition.

1. Introduction

Electrochemical capacitors (EC) have been studied by many researchers because

Nomenclatures

C_{sp}	Specific gravimetric capacitance, F/g
$(E_2 - E_1)$	Cut off potentials in CV, V
$i(E)$	Reaction current, A
m	Active mass per electrode , g
t_1	Pulse width, s
t_2	Pulse separation time, s
v	Scan rate, V/s
$\int_{E1}^{E2} i(E)dE$	Total obtained voltammetric charge, AV

it offers the intense power burst capability (i.e., high power density) and rapid chargeability [1, 2]. This is advantageous for the applications that require fast response and long energy retention [1, 2]. Under these specific applications, the EC due to its basic design (i.e., consisted of a pair of parallel plates separated by dielectrics) could be developed as a compact energy backup for portable electronic appliances [3]. The currently dominant energy storage device such as lithium ion battery has a high-energy density and is larger in size and then the EC for the same power capacity, but has shortcomings in low power density and poor energy retention [2, 3]. The recent development of EC may soon bridge the energy density-power density gap for some commercial application [2]. Likewise, EC and battery can work together as the complimenting technologies for example in the China hybrid buses, where EC operates during breaking and acceleration, with battery is used to sustain the energy need of the bus [2].

An EC consisted of active electrode materials that coated on a pair of the metallic collectors. The active electrode materials is the main contributing factors to improve the energy density of the EC, in additional to the deposition techniques and electrolytes [3, 4]. Currently, many of the EC's active electrode materials are made from the carbon phases that include graphite, graphene, activated carbon, and CNT [5]. These carbon materials have unique properties, such as good electrical, mechanical, chemical and thermal properties. The CNT has a very large specific surface area which helps to increase the EC's specific electrochemical energy storage capacity [4, 6]. CNT is widely used for the EC's electrode material due to the established synthesis process and good electrical conductivity [5].

There are attempts to replace the carbon active materials with new materials. Metal-organic frameworks (MOFs), which are extremely porous, sponge-like structures is a potential candidate because they conduct ions (i.e., through atoms or molecules) very well and have a very large surface area, far exceeds that of activated carbons [1]. Nevertheless, these carbon materials were still a leading active electrode materials for the ECs due to the established synthesis process and materials properties [5]. Furthermore, there is a continuous effort to synthesize the carbon electrode materials in a large scale from the different means and resources to reduce the materials cost [5].

Electrophoretic deposition (EPD) technique was used to deposit CNTs electrode materials due to its simplicity of set-up and its control flexibility [7, 8], as compared to the other conventional techniques such as chemical vapour deposition (CVD) [9, 10] and arc discharge [11, 12]. Previous studies showed the

pulsed EPD of CNT improves the CNTs' coating density by reducing bubble formation caused by electrolysis and particles aggregation due to the electroosmosis effect [7, 13]. Furthermore, the pulsed mode enables the vertical alignment of CNTs [7]. However, the increase of pulsed mode EPD's pulse frequency (i.e., at high frequency range) reduces the deposit yield due to a lower pH change near the depositing electrode [7, 13-15]. It is believed that the yield gain can be improved by the increase of pulse width (equivalent to the EPD time), as well as the optimization of well-dispersed suspension formulation and applied voltage [13, 16-18].

To the best of the authors' knowledges, no study has investigated the effect of EPD's pulse separation time (voltage OFF duration) on the deposition of carbon materials particles. Inertia force on the migrating particles is an important driving force for the particles movement. For example, when the voltage decreases drastically from nonzero to zero (voltage ON to voltage OFF), the accelerated particles take some time to come to a stop [13]. A longer pulse separation time may provide time for the migrating particles to adjust into the streamline flow, which is good for the uniform deposition [7]. In addition, the pulse separation time reduces Joule heating effect created by the high applied voltage [13]. The optimization of pulsed EPD process in terms of pulse separation time using an established formulation is pursued for the EC development as it provides a faster solution to improve the performance of carbon-based EC. EPD utilizes a long pulse width (voltage ON time) and pulse separation time (with durations in minute range) enables the simple EPD set up that does not require the integration of a function generator [13].

In this respect, this paper reports the deposit yield, microstructural and crystalline structure results of pulsed EPD of CNT coatings with different pulse separation times and applied voltages. Finally, the effect of the EPD's pulse separation time on the electrochemical performance of EC is discussed.

2. Experimental Details

0.4 mg/mL CNT particles suspensions were prepared by the mechanical mixing of CNT powder (multi-walled, 7-15 nm × 0.5-10 μm, SSA 2200 m^2/g, as provided by Sigma-Aldrich, 412988) in a pure isopropanol medium. $Mg(NO_3)_2$ charging additive and polyvinylpyrrolidone (PVP) binder were added at 10 wt% from the CNT particles basis. This procedure was followed by an ultrasonication in the ambient environment for 20 min to achieve a homogeneous dispersion. Microstructure of the CNT was reported in our earlier publication [4].

YEF50-grade Ni-Fe alloy sheet (thickness = 0.2 mm, Hitachi Metals Ltd) were cut into 15 mm diameter circular substrate and then rinsed with distilled water. The cathodic substrate was positioned parallel to the graphite counter electrode (rod diameter = 6 mm, Gamry Instruments) at 20 mm separation. DC voltage was supplied by an electrophoresis power supply (model: EC1000XL, Fisher Scientific) according to the voltage illustrated in Fig. 1. During the EPD, four voltage pulses with total deposition time of approximately 10 min (~2.5 min × 4 pulses, inclusive of voltage ramp-up time) was applied on each sample. DC voltages of 20, 50 and 80 V at different pulse separation times (i.e., 30, 40 and 50 s) were conducted. Prior to the EPD process, the suspensions underwent magnetic

stirring for 60 min. After the EPD, the coated samples were removed from the suspension and then dried horizontally in an ambient environment for 24 hr.

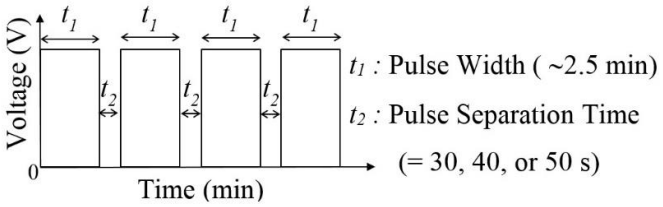

Fig. 1. Pulsed voltage-time profile of pulsed EPD used to deposit CNT coatings.

The sample's weight gain after the EPD was measured using a high precision weighing balance (0.01 milligram precision, Mettler Toledo) after air dried at 120°C for 2 hr. The deposit yield was computed from the weight difference between the deposited and blank Ni-Fe sheets. Surface microstructures of the deposited layers were then captured using scanning electron microscopy (scanning electron mode, accelerating voltage = 15 kV, Model: Evo 50, Carl Zeis AG). Raman spectroscopy (laser spot size = 1 μm, exposure time = 1 s, accumulation = 10 times, 4 mW laser power, laser beam wavelength = 532 nm, solid state laser, model: uniRAM-3500) was used to characterize the extent of graphitic carbon within the CNT coating.

Performance of the EPD-derived EC was characterized using a cyclic-voltammetry (CV) set up using a two-electrodes system powered by a potentiostat (Model: PGSTAT 204, AutoLab). The EC was constructed using a pair of the CNT coated samples (as shown in Fig. 2). Prior to the assembly, the coated samples were immersed into the potassium hydroxide (KOH) electrolyte and were uniaxially pressed up to 2000 psi. A polypropylene plate (25 μm thickness, Celgard) immersed in 1-ethyl-3-methylimidazolium bis (trifluoromethylsulfonyl) imide or [EMIM][Tf2N] IL (from Takumi Giken) was used as a separator between the electrodes. The chemical formula of the [EMIM][Tf2N] is $C_8H_{11}F_6N_3O_4S_2$.

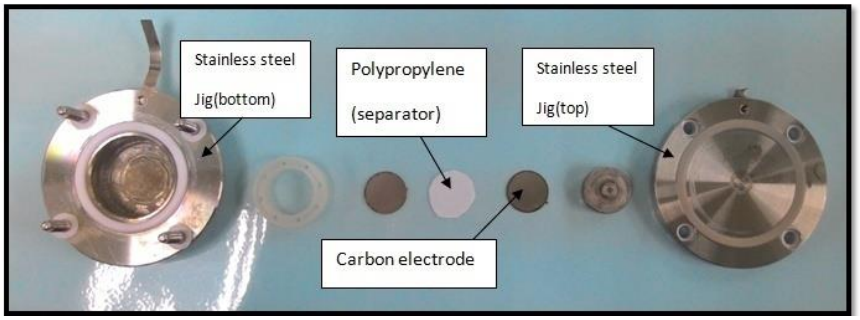

Fig. 2. EC cell construction consists of CNT deposited on Ni-Fe alloy sheet (labeled as carbon electrode).

CV curves were recorded at a scan rate of 1 mV/s between 0 and 1 V potential range. Specific gravimetric capacitance (C_{sp}) was calculated using the following equation [4, 19]:

$$C_{sp} = (\int_{E_1}^{E_2} i(E)(dE)/2(E_2 - E_1)mv \quad (1)$$

where E_1 and E_2 are the cut off potentials in CV, *i(E)* is the reaction current, *m* is the active mass per electrode, *v* is the scan rate. $(E_2 - E_1)$ is the width of CV's potential window, and $\int_{E1}^{E2} i(E)dE$ is the total obtained voltammetric charge which is obtained from the mathematical integration of positive (charge) and negative (discharge) scans in the CVs.

Finally, galvanostatic charge/discharge experiments were performed using Autolab PGSTAT 204 at constant current density of 2 mA/cm^2 with a 1.0 V potential window set-up.

3. Results and Discussion

3.1. CNT deposition yield vs. applied voltage

CNT samples exhibited three different deposit yield trends against the applied voltage (see Fig. 3). The 30 s sample shows a linear yield increase in the studied voltage range, thus was consistent with the Hamaker's law [20]. Whereas, the 40 s sample shows a nonlinear yield curve with a higher yield increase rate at the 20-50 V range, but decreased later at the 50-80 V range. The 50 s sample however exhibited constant yields at ~0.11 mg/cm^3 from 20 to 50 V and was followed by a subsequent yields drop at 50-80 V range. The 50 s sample's yield was relatively higher than the 30 s and 40 s samples at 20 V.

CNT's deteriorating yield trends were explained using DLVO theory and electric double layer (EDL) compression mechanism of the depositing particles during EPD [13, 21]. The explanation was proposed due to significant deposition of CNT particles agglomerates as shown by SEM micrographs (to be discussed later). Basically, EDL formed around the CNT particles when were suspended in a liquid medium. EDL was formed when nearby negative charged free ions were attracted to the positively charged CNT particles, forming a first ionic layer. This was followed by the second ionic layer formed by positively charged free ions. The mutual repulsive EDL maintained the particles in a stable dispersion. As voltage was applied (during the voltage ON time), EDL-electric field interaction induced the electrophoretic mobilities of the CNT particles toward the cathode. This distorted and compressed the particles' EDL. The EDL compression was subsequently weakened the CNT particles' repulsive electrostatic forces [13, 21]. Thus, the particles' attractive Van der Waals forces became dominant, causing the particles agglomeration [13, 21]. Nevertheless, the agglomerated CNT particles remained suspended during the EPD because of the anisotropic structure and a small weight (with typical density of 0.11 to 0.16 g/cm^3) [22]. The large surface area anisotropic structure CNT with negligible gravity influence made the agglomerated CNT particles become more stable than the metal and ceramic particles [21]. It is likely the CNT particles had a higher probability than ceramic particles to form agglomeration prior to EPD process. This was because of the dominancy of van der Waals attraction and particle entanglements of the former.

As the applied voltage increased, more CNT particles agglomerates were deposited at faster rate, creating more disorganized particle agglomerates coating. A longer pulse separation time created more particles agglomerates for the EPD process, resulting in more agglomerates deposition. Due to the irregular particles

arrangement of the deposited agglomerated particles, their interparticle bonding were weak, resulted in the yield loss through CNT coating disintegration during EPD. Instead of observing yield gain with the increasing voltage, the CNT's yield dropped at high voltage (i.e., 50 and 80 V) and high pulse separation time (i.e., 40 and 50 s), thus did not exhibit Hamaker's law. Electrochemical capacitor (EC)'s performance correlates with the CNT coating thickness. Our previous publication showed thick CNT coating is required to increase the electrochemical capacitor's performance [4]. The largest CNT thickness was obtained by conventional (i.e., continuous) EPD at 80 V. The microstructure and crystal structure of the CNT coating deposited at 80 V using pulse and continuous EPD were investigated to improve the CNT coating properties for EC.

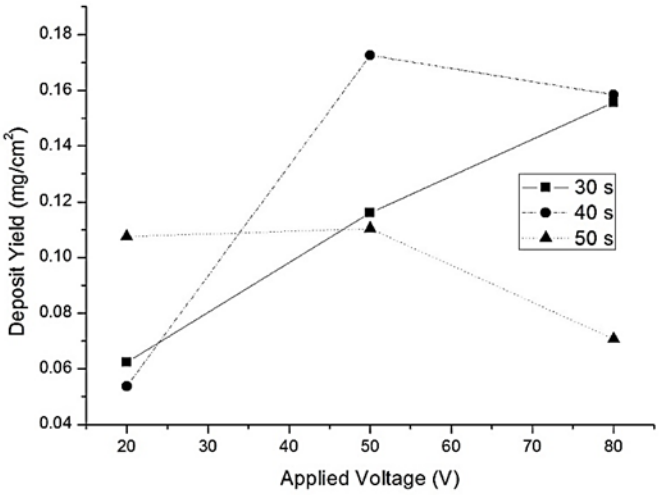

Fig. 3. Deposit yield versus applied voltage of CNT coatings deposited at different pulse separation times.

3.2. Microstructural analysis of deposited CNT

Investigations on the surface microstructure of the deposited CNT particles were performed to shed light on the cause of the non-Hamaker's law behaviour of the deposit yield. Surface micrographs of CNT coatings deposited at 80 V using a longer pulse separation time (Figs. 4 and 5) exhibited higher degree of porosity on the coating. The decreasing density of the coating validated the deposit yield drop at the longer pulse separation time (refer Fig. 4).

Large voids were observed arranged in the parallel arrays in the 50 s sample. The void size is ~6.5 μm, about the size of the deposited agglomerates observed in 30 and 40 s samples. This suggests the observed voids were created after the detachment of deposited agglomerates. This mechanism is identified by the current study as coating disintegration process. It was speculated that a similar coating disintegration mechanism may occur at a smaller scale in the 30 s and 40 s samples. Thus, the void formation became less obvious than the 50 s sample. However, a microstructural comparison of the pulsed EPD samples with the continuous EPD sample (refer to Fig. 4) clearly showed a denser coating microstructure in the continuous sample. The observed hump-like microstructures, Fig. 4(d), was probably formed by the deposition of CNT particles on the deposited agglomerates.

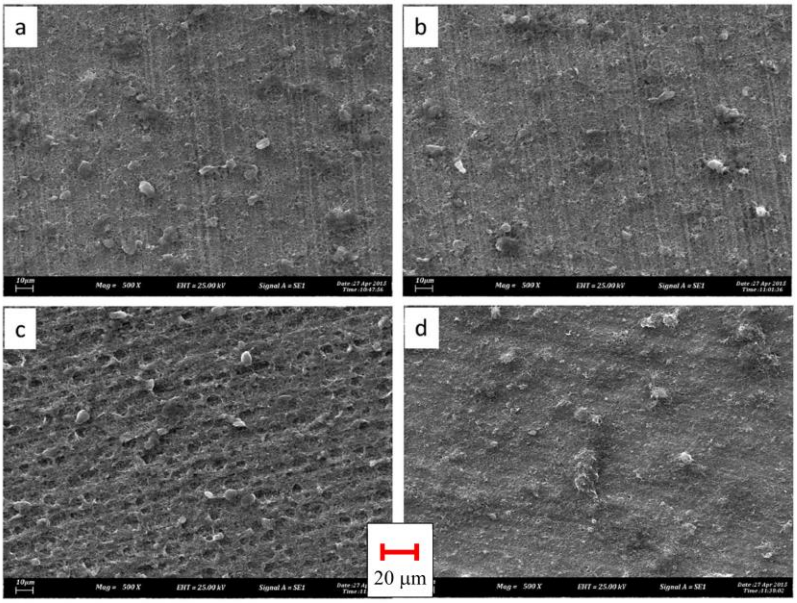

Fig. 4. Low magnification SEM micrographs of agglomerates and pores on the CNT coating surface prepared by pulsed EPD at 80 V and pulse separation time of: (a) 30 s, (b) 40 s, and (c) 50 s at 80 V. CNT coating prepared by continuous EPD is shown in (d).

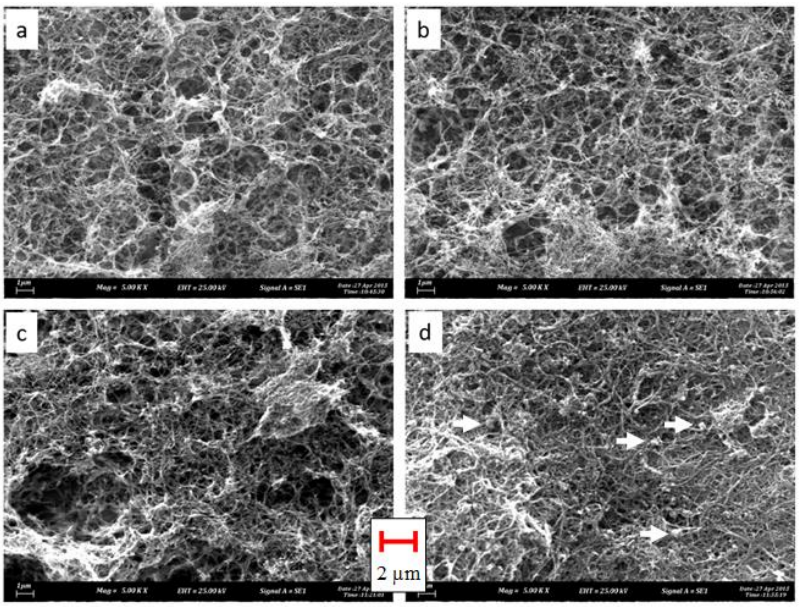

Fig. 5. High magnification SEM micrographs show CNT arrangement deposited by pulsed EPD at 80 V and pulse separation time of: (a) 30 s, (b) 40 s, and (c) 50 s. CNT coating prepared by the continuous EPD is shown in (d). Spherical particles (as shown by arrows) were found distributed randomly in the coating.

3.3. Structural properties analysis by Raman spectroscopy

Graphitic structure of the CNT coatings prepared at different pulse separation times were investigated using Raman spectra (Fig. 6). Two major peaks were observed in the deposited CNT coatings. For the continuous EPD mode samples, the D- and G-band peaks were located at 1340 and 1575 cm^{-1} respectively. When pulsed EPD was applied, G-band peaks positions was shifted to 1570 cm^{-1}. The D-band position was remained at 1340 cm^{-1}. The G-band peak was shifted toward lower Raman shift values because of an increase of vibrational state of the graphitized carbon structure [23]. The change in the vibrational state was caused by the structural attachment of non-carbon atoms onto the carbon structure [24, 25]. Since peak shift only observed in the G-peak, this may suggest the non-carbon atoms tend to attach to the graphitic CNT structure. It is also possible that the peak shift was corresponded to structural attachment by the chemicals additives of the EPD suspension (such as PVP or $Mg(NO_3)_2$). However, a further study is required to confirm the mechanism.

On the other hand, deposited samples exhibited higher Raman peaks intensity at a longer pulse separation time. The Raman peak intensity of the CNT deposits were determined by the laser scattering at the analyzed coating area [23]. Since CNT coatings deposited by the different pulse separation times have completely different surface microstructures (see Figs. 4 and 5), the cause of peak intensity increase could not be established. Consequently, the G- over D-band peaks ratio (i.e., I_G/I_D ratio) was computed to investigate the extent of structural defects in the deposited CNTs [26, 27]. Theoretically, D-band peak intensity is equivalent to the carbon defects concentration in the CNT crystal structure. The defects are associated with the vacancies and carbonaceous impurities that destroy the graphitic symmetry of the CNT crystal structure (i.e., the graphitic amount is represented by the G-band peak) [26, 27].

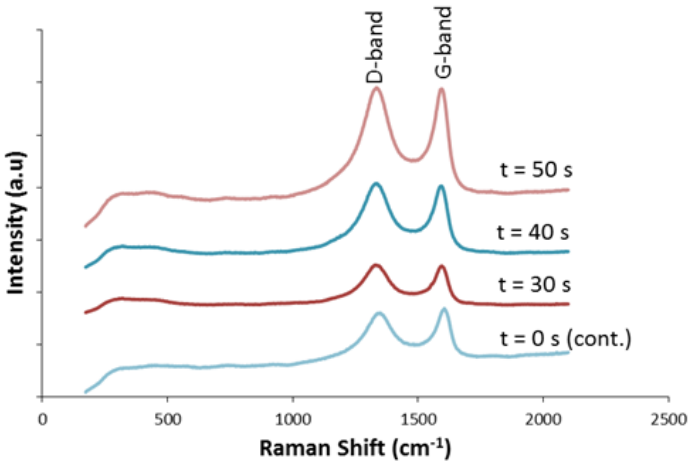

Fig. 6. Raman spectra of CNT deposit formed by pulsed EPD at different pulse separation time (*t*= 0 s refers to deposit formed by continuous EPD, applied voltage = 80 V).

Figure 7 shows the I_G/I_D ratios of the CNT coatings increased with a longer pulse separation time. A higher jump of I_G/I_D ratio was observed for the CNT

coatings when EPD using continuous mode was switched to the pulsed mode. This I_G/I_D ratio trend suggests a drastic increase (i.e., by 38%) of graphitic concentration because of the pulsed EPD. A subsequent but gradual increment of the graphitic concentration by 4% was observed when the pulse separation time increased from 30 to 50 s. The gradual increase of graphitic concentration in the pulsed EPD samples was explained the agglomerates disintegration from the CNT coatings (as suggested by the Fig. 4). The agglomerates disintegration happened concurrently with the increase of the graphitic concentration, suggesting the nongraphitic carbons were removed as part of the disintegrated agglomerates. This is also implied a significant nongraphitic carbon was participated in the particles agglomeration.

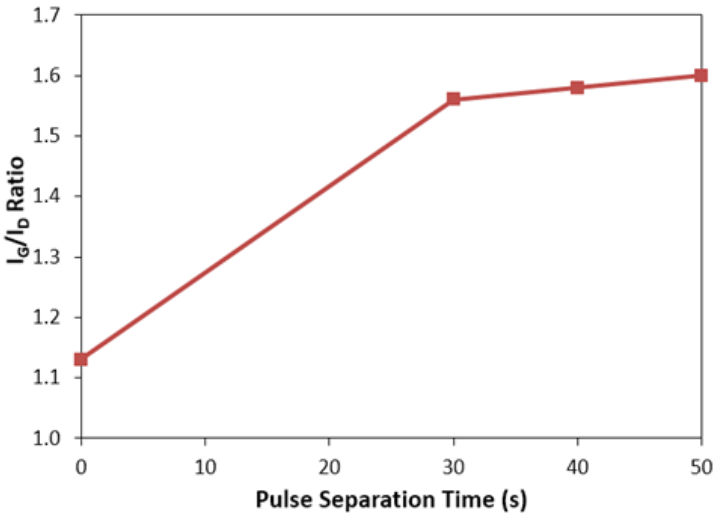

Fig. 7. G-band /D-band peak intensity ratio of CNT coatings formed by pulsed EPD at different pulse separation time (t= 0 s refers to continuous EPD sample, applied voltage = 80 V).

3.4. Electrochemical performance of electrophoretically-deposited CNT electrode

In order to investigate the effect of pulsed EPD's pulse separation time on the EC performance, CV curves (see Fig. 8) related to the CNT coatings prepared by the continuous and pulsed EPD (i.e., at 30 and 40 s) were compared. All the CV curves show leaf-shapes as the evidence of EDLC-type of EC and there is no redox peak appeared in the CV [19]. This indicates the EC is free from chemical reactions and /or is purely based on the electrostatic mechanism. The highest specific capacitance (C_{sp}) was obtained by the 30 s sample at ~170 F/g, followed by the 40 s and continuous mode samples at ~55 F/g and ~69 F/g respectively.

A jump in the C_{sp} for the 30 s sample is attributed to a higher graphitic carbon concentration (as shown by the Raman results) which provided better ion accessibility into the CNT coating [19]. However, the pulsed EPD generated more porous coating microstructure and lower yield as the pulse separation time increased to 40 and 50 s (as shown in the Fig. 5). The low-density coating microstructures decreased the electrical connectivity and the carbon surface area.

These hindered the corresponding electron transfer mechanism and indirectly lowered down the C_{sp} values. Due to a low carbon yield and poor coating density, the CV curve of the 50 s sample could not be obtained (i.e., the related measurement reading could not be obtained). Thus, it is concluded that the pulsed EPD could be used to increase the C_{sp} of EC by removing nongraphitic carbon deposited on the CNT coating. However, the removal of the deposited agglomerates created a poor coating density, which in turns lower the C_{sp} value of the EC samples.

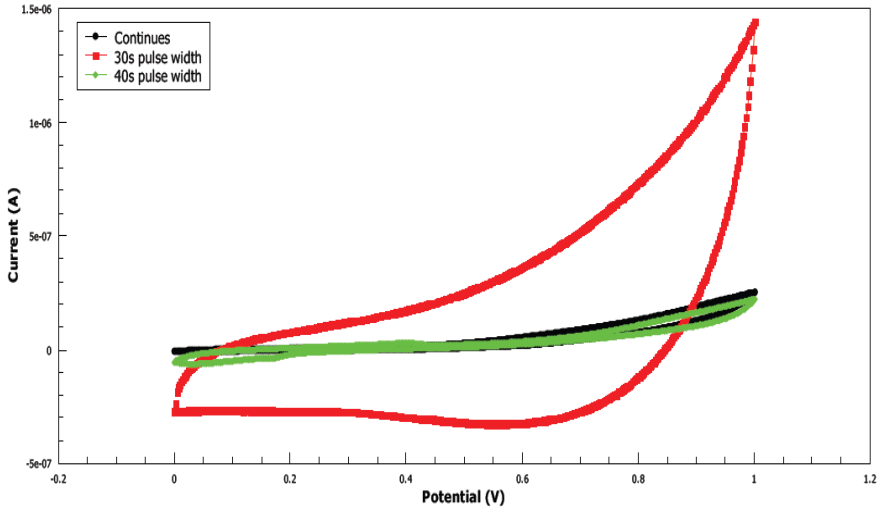

Fig. 8. CV curves of electrochemical capacitors at scan rate of 1 mV/s using CNT electrode materials deposited by continuous and pulsed EPD at 30 and 40 s (applied voltage = 80 V).

The reliability of CNT-assembled EC was measured in terms of its charge-discharge profiles (see Fig. 9). Similar to the CV result, charge-discharge profile could not be obtained for the 50 s sample due to the poor coating density (i.e., the related measurement gave an error reading). The profiles of the continuous and pulsed mode samples did not form symmetric triangular shapes due to a better discharging capability. In this case, a longer discharging than the charging time were observed. There was IR drops (i.e., ~250 mV) from the initial voltage (i.e., 1 V) due to the presence of internal resistance in the EC derived caused by the nonconductive PVP binder [19]. Thus, it is recommended that the electrolyte selection and its concentration need to be carefully tuned to reduce the internal resistance [28, 29].

30 s sample exhibited a faster charging rate but shows a slower discharging rate than the continuous EPD sample. The related EC's charging time reduced from 2.25 to 1.75 s and the discharging time increased from 4.5 s to 5 s. Nevertheless, a significantly slower discharging rate (i.e., 6.5 s) was observed for 40 s sample, while the charging profile was similar with the 30 s sample. Overall, the pulsed EPD samples recorded a faster charging and slower discharging rates than the continuous mode sample. This suggests the graphitic carbon concentration had significant influence on the charging-discharging profile. Since

the charging and discharging process of EC occurred through the absorption and release of ions from the CNT electrode, the graphitic carbon due to its higher conductivity behaviour, accelerated the ion absorption process [5]. However, the ion absorption process was hindered by lower CNT's total surface area, caused by the yield decrease and the uneven coating (void) microstructure. Solution to these problems is by minimizing the agglomerates deposition, which could be done by the disaggregation of nongraphitic carbon from the EPD suspension before EPD process begin. It is also possible that the agglomerates formation could be reduced through the suspension's formulation optimization, particularly the addition level of suspension additives (such as electrolyte salt and binder) and the improvement of the EPD process.

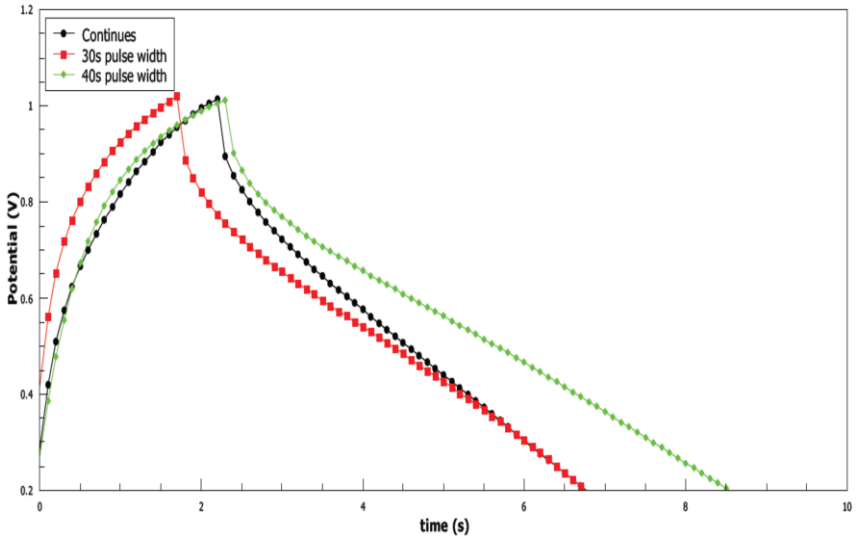

Fig. 9. Charge discharge profiles of electrochemical capacitors at 2 mA/cm^2 current using CNT electrode materials deposited by continuous and pulsed EPD at 30 and 40 s (applied voltage = 80 V).

4. Conclusions

This paper presents a comparative study on the coating characteristics of carbon nanotube (CNT) deposited by the continuous and pulsed electrophoretic deposition (EPD) processes. The characteristics were used to explain the effects on the assembled electrochemical capacitor (EC)'s performance in terms of the specific capacitance and charge-discharge profile. CNT yield of the pulsed EPD exhibited a nonlinear and decreasing trend at the increasing voltage when applied at pulse separation times of 40 and 50 s. The yield decrease was due to agglomerates disintegration from deposited CNT coating during EPD process. When the applied voltage was set at 80 V, their coatings' density and the surface areas were less than the continuous EPD samples'. A lower coating density reduced the electron transfer rate in the EC's CNT electrodes, thus detrimental to the ECs' specific capacitances and charging-discharging capability. Nevertheless, pulsed EPD samples had higher graphitic carbon concentrations than the continuous EPD. A higher electron transfer rate was expected in an EC assembled

with high graphitic CNT electrodes because of better electrical conductivity. This contributed to a better EC performance when pulse separation time of 30 s was used. The specific capacitance increased by 150%, and the EC's charging time decreased and discharging time increased by 20% and 10% respectively when compared to the continuous EPD samples. However, the detrimental effect of poor coatings' density had outweighed the positive influence of high graphitic CNT concentration in the EC performance using pulse separation times of 40 and 50 s. Thus, their specific capacitances and charging-discharging capabilities were inferior to the EC of the continuous EPD samples. It is recommended that further investigation on the suspension formulation and the voltage-time profile for the pulsed EPD of CNT are required to minimize the CNT agglomeration and maintain the CNT coating density and yield.

Acknowledgements

The authors would like to thank Universiti Teknikal Malaysia Melaka and Ministry of Higher Education Malaysia for the financial supports (Grant No.: PJP/2013/FKP(3B)/S01160 and PJP/2013/FKP/PROTOTAIP/S01291).

References

1. Sheberla, D.; Bachman, J.C.; Elias, J.S.; Sun, C.-J.; Yang, S.-H.; and Dinca, M. (2016). Conductive MOF electrodes for stable ECs with high areal capacitance. *Nature Materials*, Advance Online Publication.
2. Miret, S. Storage Wars: Batteries vs. ECs. *Berkeley Energy and Resources Collaborative*, 10 November 2013.
3. Diaz, R.; and Doherty, A.P. (2016). Carbons, ionic liquids and quinones for electrochemical capacitors. *Frontiers in Materials*, 3, 1-7.
4. Talib, E.; Lau, K.T.; Zaimi, M.; Bistamam, M.S.A.; Manaf, A.; Syafira, N.; Seman, R.; Amalina, R.N.; Zulkapli, N.N.; and Azam, M.A. (2015). Electrochemical performance of multi walled carbon nanotube and graphene composite films using electrophoretic deposition technique. *Applied Mechanics and Materials*, 761, 468-472.
5. Gu, W.; and Yushin, G. (2014). Review of nanostructured carbon materials for electrochemical capacitor applications: advantages and limitations of activated carbon, carbide ‐ derived carbon, zeolite ‐ templated carbon, carbon aerogels, carbon nanotubes, onion ‐ like carbon, and graphene. *Wiley Interdisciplinary Reviews: Energy and Environment*, 3(5), 424-473.
6. Wu, Q.; Xu, Y.; Yao, Z.; Liu, A.; and Shi, G. (2010). ECs based on flexible graphene/polyaniline nanofiber composite films. *ACS Nano*, 4(4), 1963-1970.
7. Chávez-Valdez, A.; and Boccaccini, A.R. (2012). Innovations in electrophoretic deposition: Alternating current and pulsed direct current methods. *Electrochimica Acta*, 65, 70-89.
8. Lau, K.-T.; Razak, M.H.R.A.; Kok, S.-L.; Zaimi, M.; Rashid, M.W.A.; Mohamad, N.; and Azam, M.A. (2015). Electrophoretic deposition and heat treatment of steel-supported PVDF-graphite composite film. *Applied Mechanics and Materials*, 761, 412-416.

9. Roy, S.; Bajpai, R.; Soin, N.; Roy, S.S.; McLaughlin, J.A.; and Misra, D.S. (2014). Diameter control of single wall carbon nanotubes synthesized using chemical vapor deposition. *Applied Surface Science*, 321, 70-79.
10. Manaf, N.S.A.; Bistamam, M.S.A.; and Azam, M.A. (2013). Development of high performance electrochemical capacitor: A systematic review of electrode fabrication technique based on different carbon materials. *ECS Journal of Solid State Science and Technology*, 2(10), M3101-M3119.
11. Su, Y.; and Zhang, Y. (2015). Carbon nanomaterials synthesized by arc discharge hot plasma. *Carbon*, 83, 90-99.
12. Arora, N.; and Sharma, N.N. (2014). Arc discharge synthesis of carbon nanotubes: Comprehensive review. *Diamond and Related Materials*, 50, 135-150.
13. Ammam, M. (2012). Electrophoretic deposition under modulated electric fields: A review. *RSC Advances*, 2(20), 7633-7646.
14. Neirinck, B.; Van Der Biest, O.; and Vleugels, J. (2013). A current opinion on electrophoretic deposition in pulsed and alternating fields. *The Journal of Physical Chemistry B*, 117(6), 1516-1526.
15. Wang, S.-C.; and Huang, B.-C. (2008). Field emission properties of Ag/SiO_2/carbon nanotube films by pulsed voltage co-electrophoretic deposition. *Thin Solid Films*, 517(3), 1245-1250.
16. Benko, A.; Przekora, A.; Wesełucha-Birczyńska, A.; Nocuń, M.; Ginalska, G.; and Błażewicz, M. (2016). Fabrication of multi-walled carbon nanotube layers with selected properties via electrophoretic deposition: physicochemical and biological characterization. *Applied Physics A*, 122(4), 1-13.
17. Lim, J.; Jalali, M.; and Campbell, S.A. (2015). Electrophoretic deposition of single wall carbon nanotube films and characterization. *MRS Proceedings*, 1752, 59-63.
18. Wang, H. (2009). Dispersing carbon nanotubes using surfactants. *Current Opinion in Colloid & Interface Science*, 14(5), 364-371.
19. Azam, M.A.; Dorah, N.; Seman, R.N.A.R.; Manaf, N.S.A.; and Kudin, T.I.T. (2015). Electrochemical performance of activated carbon and graphene based EC. *Materials Technology*, 30(sup2), A14-A17.
20. Hamaker, H.C. (1940). Formation of a deposit by electrophoresis. *Transactions of the Faraday Society*, 36, 279-287.
21. Lau, K.-T.; and Sorrell, C.C. (2013). Effect of charging agents on electrophoretic deposition of titanium particles. *Journal of The Australian Ceramics Society*, 49(2), 104-112.
22. Smith, W.F.; and Hashemi, J. (2006). *Foundations of Materials Science and Engineering*. New York, McGraw Hill
23. Bowley, H.J.; Gerrard, D.L.; Louden, J.D.; Turrell, G.; Gardiner, D.J.; and Graves, P.R. (2012). *Practical Raman Spectroscopy*, Springer Science & Business Media.
24. Kuo, C.-T.; Wu, J.-Y.; and Lu, T.-R. (2001). Synthesizing crystalline carbon nitrides by using two different bio-molecular materials. *Materials Chemistry and Physics*, 72(2), 251-257.
25. Roh, J.-S. (2008). Structural Study of the Activated Carbon Fiber using Laser Raman Spectroscopy. *Carbon Letter*, 9(2), 127-130.

26. Steven, E.; Saleh, W.R.; Lebedev, V.; Acquah, S.F.; Laukhin, V.; Alamo, R.G.; and Brooks, J.S. (2013). Carbon nanotubes on a spider silk scaffold. *Nature Communication*, 4, Article number: 2435 (2013).
27. Osswald, S.; Flahaut, E.; Ye, H.; and Gogotsi, Y. (2005). Elimination of D-band in Raman spectra of double-wall carbon nanotubes by oxidation. *Chemical Physics Letters*, 402(4-6), 422-427.
28. An, K.H.; Jeon, K.K.; Heo, J.K.; Lim, S.C.; Bae, D.J.; and Lee, Y.H. (2002). High-capacitance EC using a nanocomposite electrode of single-walled carbon nanotube and polypyrrole. *Journal of The Electrochemical Society*, 149(8), A1058-A1062.
29. Halper, M.S.; and Ellenbogen, J.C. (2006). *ECs: A brief overview*. The MITRE Corporation, McLean, Virginia, USA, 1-34.